RAPID COMMUNICATIONS

PHYSICAL REVIEW A VOLUME 43, NUMBER 10 15 MAY 1991

Vector statistics of multiply scattered waves in random systems

S. M. Cohen, D. Eliyahu, I. Freund, and M. Kaveh
Department of Physics, Bar-Ilan University, Ramat-Gan 52100, Israel
(Received 13 November 1990)

Statistical distribution functions are derived for the polarization of optical waves transmitted through a random medium. Excellent agreement is obtained with experiment. Our most significant result is the distribution function for the ellipticity ϵ, the ratio between the major and minor axes of the elliptically polarized scattered light. This has a maximum at $\epsilon=0$ and vanishes for $\epsilon=1$, indicating that linear polarization is the most probable state and that circular polarization has vanishing probability. The averaged ellipticity is found to be $\langle\epsilon\rangle=1-\ln 2=0.307$.

The statistical properties of scattered waves from random media have recently attracted much theoretical[1-7] and experimental[8-11] interest. Interference between different Feynman trajectories leads[3-7] to long-range intensity fluctuations, which were recently confirmed experimentally[10,11] for narrow samples. For wide samples, however, the intensity fluctuations at a given point are governed by Rayleigh statistics, $P(I_i)=\langle I_i\rangle^{-1}\exp(-I_i/\langle I_i\rangle)$, where I_i is the intensity of each component of the electric field. An interesting question is how to characterize the statistical properties of the *vector* nature of the scattered optical waves. When an incident linearly polarized wave undergoes a single scattering it remains linearly polarized. The new feature of multiple scattering is to change its polarization state in a statistical manner. This property is demonstrated in Fig. 1, where we show a typical picture of speckle spots caused by scattered optical waves, with the polarization state of a speckle (coherence area) being measured via the rotation of a polarizer. At some speckle spots, the wave remains linearly polarized, whereas at other spots, it becomes circularly polarized, and at still other speckle spots, it is elliptically polarized. Thus, the statistical distribution of this elliptically polarized scattered light is an interesting unresolved problem. The same question can also be asked for scattering of electrons or neutrons from random systems where the spin replaces the role of the polarization.

Here, we study the statistical distribution of the polarization state of multiply scattered optical waves. We determine the probability distribution $P(\epsilon)$ for the ellipticity ϵ of the elliptical polarization state of the light. This distribution has its maximum at $\epsilon=0$, which implies that the scattered wave favors a nearly linearly polarized state. The averaged ellipticity was found to be $\langle\epsilon\rangle=1-\ln 2=0.307$. We have also calculated the distribution functions $P_a(I_a)$ and $P_b(I_b)$ for the intensities along the major and minor axes, a and b, of each ellipse and the distribution $P_\theta(\theta)$ of the tilt of these principal axes relative to the incident polarization. All these vector field distributions deviate markedly from the Rayleigh statistical law. In particular, $P_a(I_a\to 0)\propto I_a$, $P_b(I_b)$ *diverges* as $I_b^{-1/2}$, while the joint probability $P(I_a,I_b)$ *vanishes* when $I_a=I_b$, indicating a vanishing probability for circular polarization. These distribution functions are all calculated as a function of the depolarization of the multiply scattered light $\rho=\langle I_y\rangle/\langle I_x\rangle$, with x the direction of the incident polarization, and were found to be in agreement with our experiment.

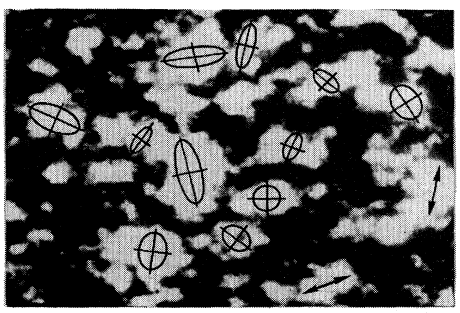

FIG. 1. Speckle pattern for multiply scattered optical waves, showing the elliptical polarization of various speckle spots.

Suppose an incident wave with electric field $\mathbf{E}_{\rm in}=E_0\hat{\mathbf{x}}$ propagates in a random medium in the z direction and due to multiple scattering is scattered into all directions. We concentrate on directions in the near vicinity of the z direction, which implies that the scattered wave is given by $\mathbf{E}=E_x\hat{\mathbf{x}}+E_y\hat{\mathbf{y}}$. The real and imaginary parts of E_x and E_y each obey Gaussian statistics. This follows from the central limit theorem, since each component consists of an infinite sum of partial waves which have traversed independent Feynman trajectories. From the fact that $\langle I\rangle$ and $\langle I^2\rangle$ do not depend on the direction of $\mathbf{E}_{\rm in}$ it follows that E_x and E_y are uncorrelated.[12,13] Thus, $P(E_i)$, $(i=x,y)$ is simply

$$P(E_i)=\pi^{-1}\langle|E_i|^2\rangle^{-1}\exp(-|E_i|^2/\langle|E_i|^2\rangle).$$

The vector nature of the scattered wave is therefore determined by four independent Gaussian variables ($\mathrm{Re}E_x$, $\mathrm{Im}E_x$, $\mathrm{Re}E_y$, $\mathrm{Im}E_y$). In order to specify the vector statistics of the scattered wave, we will require the statistics of the relative phase γ which is determined from $E_y/E_x=|E_y/E_x|e^{i\gamma}$. Since $\gamma=\phi_y-\phi_x$, where ϕ_i is the phase of E_i, and (ϕ_x,ϕ_y) are independent and uniformly distributed between $-\pi$ and π, the distribution function for $P(\gamma)$ is given by $P(\gamma)=(2\pi-|\gamma|)/4\pi^2$. With this, the problem reduces to one of three statistically independent variables $(|E_x|,|E_y|,\gamma)$.

We have, however, only two principal axes, a and b, along which we would like to find $P_a(I_a)$ and $P_b(I_b)$, so one might expect these to be independent. One of the main interesting results of this paper, however, is that the degree of correlation between I_a and I_b is, in fact, extremely high.

Our most general joint distribution function is

$$P(I_a,I_b,\theta;\rho)=\frac{2(I_a-I_b)(\rho+1)^2}{\pi\langle I\rangle^2(I_aI_b)^{1/2}\rho}\exp[-(I_a+I_b)(1+\rho)^2/2\langle I\rangle\rho]\cosh[R(\theta)]\,, \tag{1a}$$

where $R(\theta)=[(1-\rho^2)/\rho][(I_a-I_b)/2\langle I\rangle]\cos2\theta$, $\langle I\rangle=\langle I_a\rangle+\langle I_b\rangle$,[14] and θ is the angle between the principal axes and the (x,y) coordinate system and is restricted by $-\pi/4<\theta<\pi/4$. When (1a) is integrated over θ, the joint probability $P(I_a,I_b;\rho)$ is given by

$$P(I_a,I_b;\rho)=\frac{(I_a-I_b)(1+\rho)^2}{\langle I\rangle^2(I_aI_b)^{1/2}\rho}\exp\left[-\frac{(I_a+I_b)(1+\rho)^2}{2\langle I\rangle\rho}\right]I_0\left[\frac{(1-\rho^2)}{2\rho}\frac{I_a-I_b}{\langle I\rangle}\right], \tag{1b}$$

where I_0 is a zero-order Bessel function. The interesting feature of this distribution is that it vanishes for circularly polarized speckles where $I_a=I_b$ and it diverges for $I_b\to 0$.

From Eqs. (1a) and (1b) we are able to obtain analytical results for a variety of other important distribution functions. We first show our results for the most interesting case of complete depolarization, $\rho=1$, and compare them with the measured distributions. The distribution functions for $P_a(I_a)$ and $P_b(I_b)$ are given by

$$P_a(I_a)=\exp(-2I_a/\langle I\rangle)\{2/\langle I\rangle\exp(-2I_a/\langle I\rangle)+d(I_a)\,\mathrm{erf}[(2I_a/\langle I\rangle)^{1/2}]\} \tag{2a}$$

and

$$P_b(I_b)=P_a(I_b)-d(I_b)\exp(-2I_b/\langle I\rangle)\,, \tag{2b}$$

where

$$d(I_a)=\pi^{1/2}[(8I_a/\langle I\rangle^3)^{1/2}-(1/2I_a\langle I\rangle)^{1/2}]\,.$$

We see that $P_a(I_a)$ and $P_b(I_b)$ are very different, $P_a(I_a\to 0)\propto I_a$ whereas $P_b(I_b\to 0)\propto I_b^{-1/2}$, which is a manifestation of the high probability for a linearly polarized state.

We now compare these theoretical results with our measured distribution functions. We have measured with the aid of a He-Ne laser the scattered intensity from a $BaSo_4$ diffuse coating,[2] by determining (see Fig. 1) the elliptical polarization of each speckle spot by extending the video methods used previously.[8,9,12] In Figs. 2(a) and 2(b), we plot the measured distribution functions for the major axis, $P_a(I_a)$, and for the minor axis, $P_b(I_b)$. These distributions required the measurements of 2.88 million data points. The agreement with the theory (solid curves) is evident from the figure.

The most informative distribution function is for the ellipticity $\epsilon=(I_b/I_a)^{1/2}$ which for $\rho=1$ is found to have the surprisingly simple form

$$P_\epsilon(\epsilon)=\frac{2(1-\epsilon^2)}{(1+\epsilon^2)^2}\,. \tag{3}$$

This has its maximum value at $\epsilon=0$, vanishes at $\epsilon=1$, and yields $\langle\epsilon\rangle=1-\ln2=0.307$. In Fig. 2(c), we compare this result with the measured distribution $P_\epsilon(\epsilon)$ for $\rho=0.93$. The agreement is satisfactory and confirms that the most probable polarization is linear and the least probable polarization is circular. This can be understood from the fact that for a linearly polarized speckle, the relative phase $\gamma=0$ but the amplitudes $|E_x|$ and $|E_y|$ are arbitrary; whereas for circularly polarized speckles, the fixed phase is $\gamma=\pi/2$ but the amplitudes are restricted with the constraint $|E_x|=|E_y|$. Thus, the circular polarization has vanishingly small phase space relative to linear polarization.

We now turn to the correlations between the intensities along the principal axes of the ellipses, defined by $C_{mn}\equiv\langle I_a^mI_b^n\rangle/\langle I_a^m\rangle\langle I_b^n\rangle$. Our analytic result is

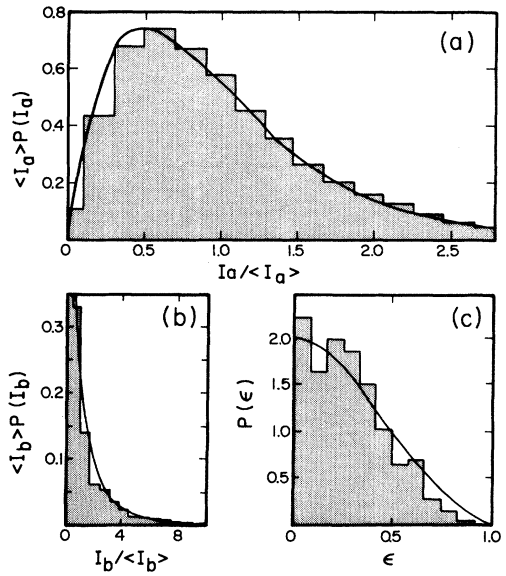

FIG. 2. Distribution functions for intensities along the major and minor principal axes of the elliptical polarization. Histograms represent experimental data obtained in reflection from $BaSO_4$ with $\rho=0.93$. The solid curves represent our theory for $\rho=1$. Note that deviations from the $\rho=1$ curves are only significant for $\rho\ll1$. (a) $P_a(I_a)$, the intensity along the major axis, with the solid curve from Eq. (2a); (b) $P_b(I_b)$, the intensity along the minor axis. The solid curve is from Eq. (2b); (c) $P_\epsilon(\epsilon)$, with $\epsilon=(I_b/I_a)^{1/2}$. The solid curve is from Eq. (3).

$$C_{mn}=\frac{4\Gamma(m+n+2)[F(m+n+2,n+\frac{3}{2})/(n+\frac{1}{2})-F(m+n+2,n+\frac{5}{2})/(n+\frac{3}{2})]}{\Gamma(m+2)\Gamma(n+2)[2F(m+2,\frac{3}{2})-\frac{2}{3}F(m+2,\frac{5}{2})][F(n+2,n+\frac{3}{2})/(n+\frac{1}{2})-F(n+2,n+\frac{5}{2})/(n+\frac{3}{2})]}, \quad (4)$$

where $F(x,y)={}_2F_1(1,x,y,\frac{1}{2})$, and ${}_2F_1$ is the hypergeometric function. As m or n increases, C_{mn} increases rapidly, indicating a surprisingly strong degree of correlation between I_a and I_b. We have measured C_{mn} and find good agreement with the result of Eq. (4). In Fig. 3, we compare theory and experiment for C_{mn} with $m,n\leq 4$. The agreement is evident from the figure, and confirms experimentally the high degree of correlation between I_a and I_b. In contrast to these strong correlations we plot in the inset of Fig. 3,

$$C'_{mn}=\frac{\langle(I_a-I_b)^m I_b^n\rangle}{\langle(I_a-I_b)^m\rangle\langle I_b^n\rangle}.$$

We see that all the points are near unity, indicating that for a given average intensity, the distribution of elliptical shapes has the property that I_a-I_b is nearly independent of I_b.

We now derive Eq. (1) and the distribution functions which follow from it for a general depolarization state ρ. The joint probability for the three independent variables $(|E_x|,|E_y|,\gamma)$ is found to factorize in the following way:

$$P(|E_x|,|E_y|,\gamma)=P_1(|E_x|)P_2(|E_y|)P_3(\gamma), \quad (5)$$

where $|E_i|^{-1}P_i(|E_i|)$ follows a Gaussian distribution and $P_3(\gamma)=(2\pi-|\gamma|)/4\pi^2$. Defining variables x and y by

$$x=I_x+I_y,$$
$$y=[(I_x-I_y)^2+4I_xI_y\cos^2\gamma]^{1/2}, \quad (6)$$

with $I_i=|E_i|^2$, we obtain the intensities (I_a,I_b) along the principal axes of the ellipses as

$$I_a=\tfrac{1}{2}(x+y),$$
$$I_b=\tfrac{1}{2}(x-y). \quad (7)$$

From Fig. 1, we see that each ellipse is tilted with an angle θ relative to the (x,y) axes. This angle is given by

$$\tan 2\theta=\frac{2|E_x||E_y|\cos\gamma}{|E_x|^2-|E_y|^2}. \quad (8)$$

From these relations, we obtain the most general distribution function $P(I_a,I_b,\theta)$ as given by Eq. (1a). Integrating over θ leads to our Eq. (1b).

From Eq. (1b), we obtain the generalized distribution function for the ellipticity $P_\epsilon(\epsilon,\rho)$ which is given by

$$P_\epsilon(\epsilon,\rho)=\frac{8(1-\epsilon^2)(1+\rho)\rho}{(1+\epsilon^2)^2\{(1+\rho)^2-[(1-\epsilon^2)/(1+\epsilon^2)]^2(1-\rho)^2\}^{3/2}}. \quad (9)$$

For $\rho=1$, Eq. (9) coincides with Eq. (3) whereas for $\rho=0$ (which corresponds to single scattering), $P(\epsilon)=\delta(\epsilon)$ which means that the ellipses degenerate into strictly linear polarization. This determines all the statistical properties of the distribution functions of the ellipses for an arbitrary depolarization ρ. From Eq. (1a) we derive $P(\epsilon,\theta,\rho)$ which can be

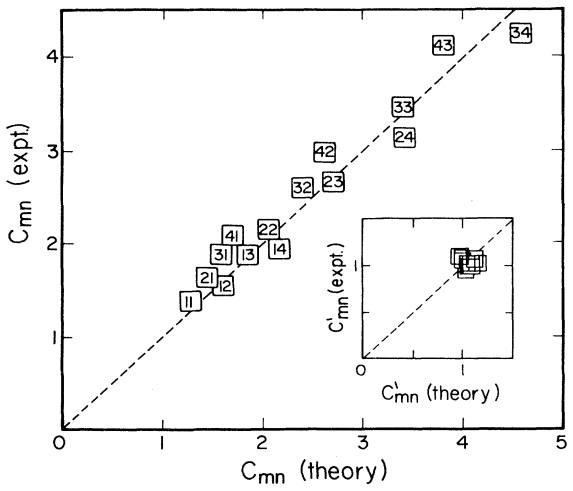

FIG. 3. The correlation functions, $C_{mn}=\langle I_a^m I_b^n\rangle/\langle I_a^m\rangle\langle I_b^n\rangle$ for $1\leq m,n\leq 4$. The experimental results for $\rho=0.93$ are plotted against the theoretical predictions of Eq. (4), $\rho=1$. The values (m,n) are listed in the squares which represent the data points. The dashed line represents perfect agreement. The strong correlations are apparent in the fact that $C_{mn}>1$. Inset: C'_{mn}, experiment vs theory (the latter are numerical results).

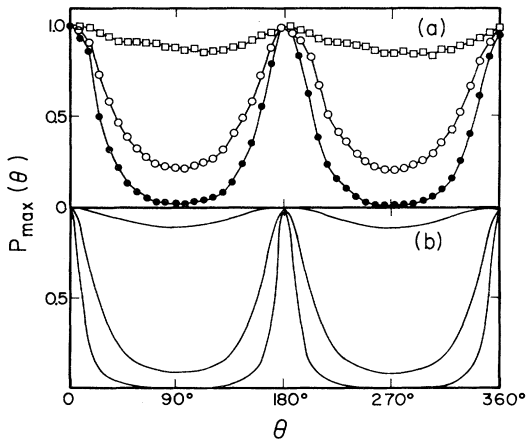

FIG. 4. The distribution function $P_+(\theta_+,\rho)$ for the angle between the major axis of the ellipse and the incoming polarization vector: (a) Experimental results in reflection; squares: $\rho=0.93$, $BaSO_4$ diffuse coating, estimated transport mean free path ≈ 5 μm; open circles: $\rho=0.2$, TiO_2 in polystyrene, estimated transport mean free path ≈ 50 μm; solid circles: $\rho=0.04$, anodized aluminum. The solid lines are guides to the eye. (b) Theoretical predictions from Eq. (11) for values of ρ matching those of the experimental curves.

decomposed into $P_+(\epsilon,\theta_+;\rho)+P_-(\epsilon,\theta_-;\rho)$ where $P_\pm(\epsilon,\theta_\pm,\rho)$ is the probability distribution when θ is measured relative to the major or minor principal axes, respectively. From the fact that $P_+(\epsilon,\theta_+;\rho)=P_-(\epsilon,\theta_-+\pi/2;\rho)$ we find

$$P_\pm(\epsilon,\theta_\pm;\rho)=\frac{8\rho(1-\epsilon^2)}{\pi}[(1+\epsilon^2)(1+\rho)\pm(1-\epsilon^2)(1-\rho)\cos2\theta_\pm]^{-2}. \tag{10}$$

We see that only for complete depolarization, $\rho=1$, is the distribution function $P(\epsilon,\theta,\rho=1)$ independent of θ and coincides with Eq. (9). This is as expected since for $\rho=1$ there is no preferred direction for the principal axes of the ellipses and their directions are uniformly distributed. As ρ decreases, this uniformity is lost and a peak is developed around $\theta=0$.

Integrating over ϵ we get,

$$P_+(\theta_+;\rho)=\frac{6a\rho}{\pi b}\left\{1-\left[\left(\frac{a}{b}\right)^{1/2}-\left(\frac{b}{a}\right)^{1/2}\right]\arctan\left(\frac{b}{a}\right)^{1/2}\right\}, \tag{11}$$

where $a=1+\rho+(1-\rho)\cos2\theta_+$ and $b=(1+\rho)-(1-\rho)\cos2\theta_+$.

In Fig. 4, we plot our experimental distribution function $P_+(\theta_+;\rho)$ for $\rho=0.93$, 0.2, 0.04, and compare it with Eq. (11). Due to noise in the experiment, which tended to obscure the angle at which the intensity of a given speckle spot peaked, the maxima are rounded compared to the theoretical curves; otherwise the agreement is quite good. We see that as ρ decreases $P_+(\theta_+)$ becomes more peaked around $\theta_+=0$.

We have also extended[15] the present method to a general outgoing wave-vector direction which forms an angle θ relative to the incident electric field $\mathbf{E}_{in}$. We find that all the present results are still valid but are rescaled by replacing ρ with $\rho^*=\rho/(\sin^2\theta+\rho\cos^2\theta)$. The consequences of this scaling will be presented elsewhere.[15]

We are pleased to acknowledge important discussions with I. Kanter. This work was supported by the Basic Research Administration of the Israel Academy of Science and Humanities, and by the Israel-U.S. Binational Science Foundation, Jerusalem.

[1]B. Shapiro, Phys. Rev. Lett. **57**, 2168 (1986).
[2]M. Kaveh, M. Rosenbluh, I. Edrei, and I. Freund, Phys. Rev. Lett. **57**, 2049 (1986).
[3]M. J. Stephen and G. Cwilich, Phys. Rev. Lett. **59**, 285 (1987).
[4]S. Feng, C. Kane, P. A. Lee, and A. D. Stone, Phys. Rev. Lett. **61**, 834 (1988).
[5]I. Edrei, M. Kaveh, and B. Shapiro, Phys. Rev. Lett. **62**, 2120 (1989).
[6]R. Berkovits, M. Kaveh, and S. Feng, Phys. Rev. B **40**, 739 (1989); R. Berkovits and M. Keveh, *ibid.* **41**, 2635 (1990); **41**, 7308 (1990).
[7]R. Pnini and B. Shapiro, Phys. Rev. B **39**, 6986 (1989).
[8]I. Freund, M. Rosenbluh, and S. Feng, Phys. Rev. Lett. **61**, 2328 (1988).
[9]I. Freund, M. Rosenbluh, and R. Berkovits, Phys. Rev. B **39**, 12403 (1989).
[10]N. Garcia and A. Z. Genack, Phys. Rev. Lett. **63**, 1678 (1989); A. Z. Genack, N. Garcia, and W. Polkosnik (unpublished).
[11]M. P. van Albada, J. F. de Boer, and A. Lagendijk (unpublished).
[12]I. Freund, M. Kaveh, R. Berkovits, and M. Rosenbluh, Phys. Rev. B **42**, 2613 (1990).
[13]J. W. Goodman, *Statistical Optics* (Wiley, New York, 1985), Chap. 2.
[14]For $\rho=1$, $\langle I_a\rangle=\frac{1}{2}(1+\pi/4)\langle I\rangle$.
[15]S. M. Cohen, M. Kaveh, and I. Freund (unpublished).

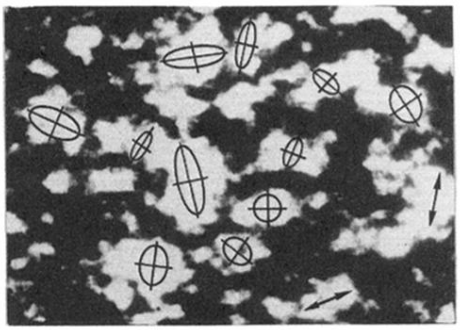

FIG. 1. Speckle pattern for multiply scattered optical waves, showing the elliptical polarization of various speckle spots.